

Mesoscopic structure of DNA–membrane self-assemblies: Microdiffraction and manipulation on lithographic substrates

Gerard C. L. Wong,^{a)} Youli Li, Ilya Koltover, and Cyrus R. Safinya
*Materials Research Laboratory, Materials Department and Physics Department,
 University of California, Santa Barbara, California 93106*

Zhonghou Cai and Wenbing Yun
Advanced Photon Source, Argonne National Laboratory, Argonne, Illinois 60439-4919

(Received 9 June 1998; accepted for publication 3 August 1998)

Using microdiffraction techniques at the Advanced Photon Source, we have found evidence for local molecular alignment within the mesoscopic fibers of DNA–cationic membrane complexes, a system originally conceived as gene delivery vectors. Furthermore, these mesoscopic structures can be manipulated by using lithographically patterned microchannel arrays, so that the optical axes of individual fibers are aligned parallel to the channels. These observations suggest that DNA–membrane complexes may have additional technological applications, such as active electrophoretic media and templates for the fabrication of semiconductor superlattices and nanoporous materials with tunable pore sizes. © 1998 American Institute of Physics. [S0003-6951(98)00640-8]

DNA–cationic membrane complexes can mimic certain characteristics of natural viruses in their ability to transport extracellular DNA across the cell membrane, and have been used as an alternative to viral DNA delivery vectors in gene therapy.¹ It has been recently demonstrated that the addition of DNA to cationic lipid mixtures can induce a topological transition from liposomes into condensed multilamellar self-assemblies, where a periodic one dimensional (1D) lattice of parallel DNA chains is confined between stacked two dimensional (2D) lipid sheets^{2,3} (Fig. 1). Moreover, by lowering the membrane's bending rigidity or by changing its spontaneous curvature, an inverted hexagonal phase with a dramatically enhanced tendency for membrane fusion can be formed, one in which DNA chains coated by lipid monolayers are packed into a 2D columnar hexagonal array.⁴ During condensation of these complexes, the cationic lipid head groups neutralize the phosphate groups on the DNA chains, effectively replacing the originally Manning condensed counterions,⁵ and consequently driving this higher order self-assembly.

These DNA–membrane complexes constitute a new class of tunable nanostructured materials with intriguing technological possibilities, in addition to its inherent fundamental interest for gene therapy and soft condensed matter physics.³ The interhelical distance between DNA chains in the 1D lattice can be tuned between 2.5 and 6.0 nm by changing the relative proportion of cationic and neutral lipids. Envisaged applications include active electrophoretic media and nanoporous materials with controllable pore sizes. It may also be possible to use these DNA–membrane complexes to template the synthesis of inorganic nanostructures (such as silicates or semiconductor superlattices) with symmetries and sizes which are currently unavailable.^{6,7} However, many of these proposed applications require control of the pore orientation. As with most of the nanoporous materials produced to date,⁸ the DNA–membrane complexes are

polycrystalline. No positional or orientational correlation between the DNA chains exists across adjacent lipid layers.

The lipid layers of the multilamellar DNA–membrane complex structure exhibit an apparent isotropic orientational distribution in small angle x-ray scattering (SAXS). However, optical microscopy has revealed that DNA–membrane complexes form birefringent globules, which aggregate into randomly oriented fibers at mesoscopic ($\sim 1 \mu\text{m}$) length scales.² A conventional SAXS measurement probes a sample area volume of $\sim 1 \text{ mm}^3$, and therefore averages over a large ensemble of fibers at different orientations. The isotropic orientational distribution of lipid layers obtained from such a measurement can be explained by a random distribution of complex orientations within the fibers, or by the orientational distribution of the fiber bundles themselves. Such information on the mesoscopic organization of these DNA–membrane complexes is crucial for an assessment of the many proposed applications outside of gene therapy. In gen-

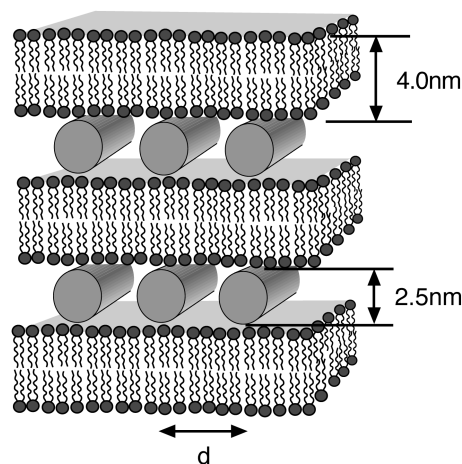


FIG. 1. A schematic representation of the lamellar DNA–cationic lipid complex. The lamellar spacing is equal to 65 Å for DOTAP–DOPC (50%–50%). The interhelical spacing of the DNA lattice d can be tuned from 25 to 60 Å by changing the DOTAP/DOPC ratio. No positional or orientational correlation between the DNA chains exists across adjacent lipid layers.

^{a)}Electronic mail: Gerard@mrl.ucsb.edu

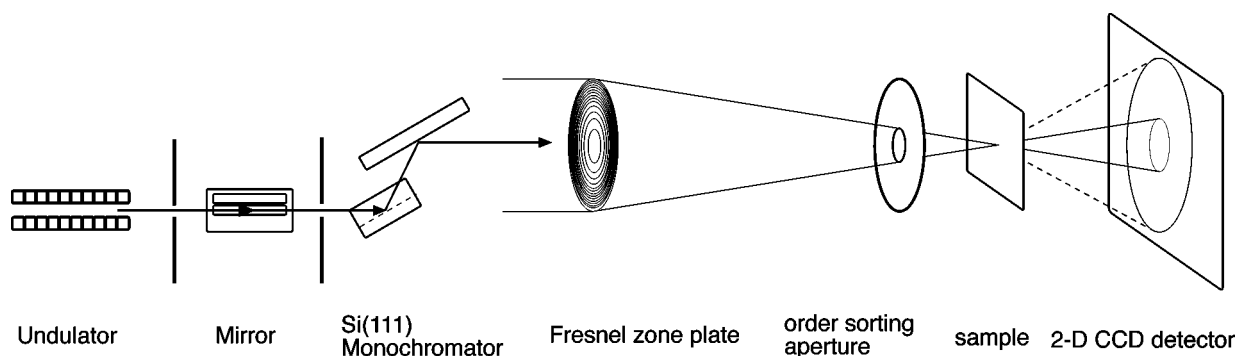


FIG. 2. A schematic representation of the microdiffraction facility at APS beamline 2-ID-D.

eral, however, the organization of local domains and any resultant modulations of the molecular structure within such DNA–membrane fibers are unknown.

In this letter, we present the first evidence for local molecular alignment within the mesoscopic fibers of DNA–membrane complexes. Using a microfocused hard x-ray beam at the Advanced Photon Source (APS), we performed a diffraction experiment within a $1\ \mu\text{m} \times 4\ \mu\text{m}$ section of a fiber bundle sample, and found it to be partially aligned. Moreover, we have demonstrated that the mesoscopic structure of DNA–membrane complex fibers can be manipulated using lithographically patterned microchannel arrays. Single fibers, each with its optical axis aligned parallel to the channel, can be made.

We examined lamellar complexes formed from λ -phage DNA (48 502 base pairs, contour length $16.5\ \mu\text{m}$), and liposomes made from a 50%–50% binary mixture of the neutral and cationic lipids, dioleoyl-phosphatidylcholine (DOPC) and dioleoyl-trimethylammonium propane (DOTAP), respectively. The mass ratio of DOTAP to DNA is 2.5, which is close to the isoelectric (charge neutral) point of the system. The samples are initially prepared on a glass cover slip, where $\sim 10\ \mu\text{l}$ of the liposome solution (25 mg/ml) is added to $\sim 10\ \mu\text{l}$ of an aqueous solution of λ -DNA (5 mg/ml). The sample is thoroughly mixed and then sealed between two $170\ \mu\text{m}$ cover slips using a $13\ \mu\text{m}$ kapton spacer ring.

The microdiffraction x-ray experiments were conducted at the 2-ID-D undulator beamline at the APS (shown in Fig. 2). Monochromatized x rays at 11.2 keV were focused to a beam size of $1 \times 4\ \mu\text{m}^2$ using a blazed Au/Si zone plate ($180\ \mu\text{m}$ diameter, 55 cm focal length, 20% focusing efficiency).⁹ The thin transmissive sample cell was positioned at the focus of the zone plate, behind an order sorting aperture of $10\ \mu\text{m}$ diameter. Due to the focusing optics, the divergence of the incident beam is 0.02° , which imposes a fundamental limit for low angle access in this zone-plate SAXS measurement. Intensities of scattered x rays were measured using a liquid nitrogen (LN_2) cooled charge-coupled device (CCD) array detector, and the resultant 2D image of the diffraction pattern covered the Q range from 0.07 to $0.53\ \text{\AA}^{-1}$. A measurement of the smectic layer spacing of the thermotropic liquid crystal 8CB (4-cyano-4'-octylbiphenyl) served as an absolute calibration for this data.

Diffraction patterns taken from two different local regions of the same DNA–membrane complex sample are exhibited in Fig. 3. The strong inner ring of scattering at $0.107\ \text{\AA}^{-1}$ corresponds to the characteristic lamellar spacing of the

complex, which is approximately equal to the thickness of the lipid membrane ($\sim 40\ \text{\AA}$) plus the diameter of a hydrated DNA chain ($\sim 25\ \text{\AA}$). The strong modulation in intensity along the ring of intensity can be seen in the adjoining χ scans. If the lamellae were randomly oriented, then an isotropic ring of scattered intensity would be observed. The present data clearly indicate partial alignment of the complex lamellae at this length scale, which is comparable to the widths of the individual fibers. The different intensity distributions for the two regions of the sample suggest that the scattering originate from differently oriented fibers. The full width at half maximum of this modulation is estimated at $\sim 60^\circ$. This represents a lower limit on the molecular alignment of an actual fiber, since the nominal thickness of the sample as determined by the kapton spacer is $13\ \mu\text{m}$, which is large enough to accommodate the thickness of several fi-

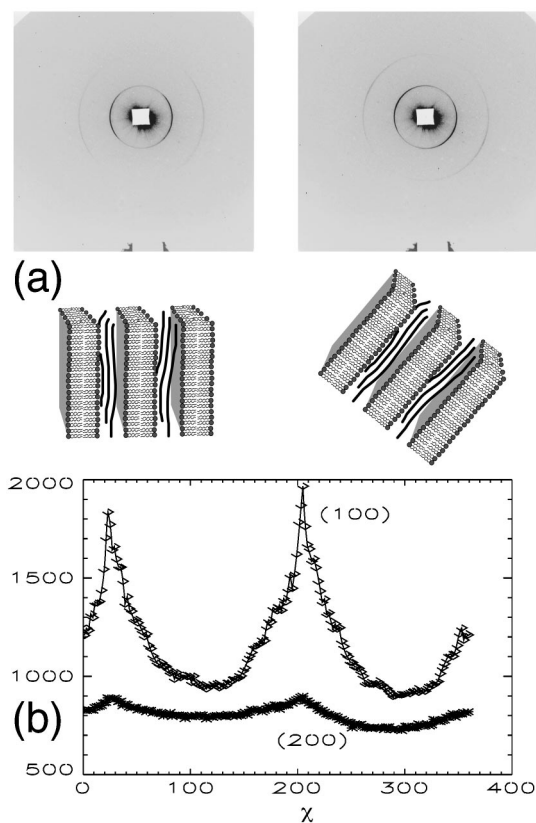


FIG. 3. (a) Diffraction patterns taken from two different local regions of the same DNA–membrane complex sample. The strong modulation in intensity along the inner ring of intensity ($\sim 0.1\ \text{\AA}^{-1}$) can be seen in the adjoining χ scans in (b).

bers. Indeed, the initial sharp decrease in intensity away from the peak maximum in χ and the asymmetry in the peak shape suggest that the scattering may be the sum of sharper components. These observations strongly suggest that the lipid lamellae of the DNA–membrane complexes in individual fibers are aligned at molecular length scales.

For this experiment, the effects of radiation damage on the DNA–membrane complex samples require scrupulous attention. The spectral brilliance of the incident beam is already $>10^{10}$ brighter than a rotating anode source. Moreover, the flux density gain from the zone plate focusing is approximately 10^3 . Radiation damage may explain the absence of the inter-DNA correlation peak, which is routinely observed in bulk samples. The sharp characteristic peak for the DNA–membrane complexes at 0.1 \AA^{-1} gradually broadens into diffuse scattering and eventually disappears for long enough exposures.

Single fibers of DNA–membrane complexes can be manipulated with the aid of lithographically generated microchannel arrays. The microchannel arrays used for this study have been fabricated on glass plates ($\sim 170 \text{ \mu m}$ thick) and Si(100) wafers ($\sim 100 \text{ \mu m}$ thick), using optical and e-beam lithography at the National Nanofabrication Users Network facility at the University of California, Santa Barbara. Reactive ion etching has been used to transfer the pattern onto the substrates. The widths of the channels in the individual arrays varied from 20 to 5 \mu m , with an average depth of 1.5 \mu m .

In order to demonstrate that single fibers of DNA–membrane complexes can be aligned, we have confined isolated fibers in individual channels of a 5 \mu m microchannel array. For the development of this procedure, we used isoelectric complexes made from λ -DNA and a 25%–75% binary mixture of DOTAP and the neutral lipid dioleoylphosphatidylethanolamine (DOPE), which form well separated fibers in the hexagonal phase.⁴ The samples are initially prepared on a glass cover slip, where the liposome solution (25 mg/ml) and the aqueous solution of DNA (0.5 mg/ml) are mixed. An isolated fiber is then drawn out of the precipitates and positioned in a glass microchannel array with 5 \mu m channels. The width of the fiber is approximately the same as the width of the channel, as is shown in Fig. 4. Images of the fiber made with polarized microscopy indicate that the fiber is strongly birefringent. Although the diffraction signal of this 5 \mu m fiber is too weak to be detected using a rotating anode x-ray source, the polarized micrographs in Fig. 4 suggest that the orientation of the complexes within the fiber is approximately homogeneous along the length of the fiber ($>2 \text{ mm}$). Compared to the randomly distributed fiber sample above, such oriented fibers are expected to exhibit much stronger intensity modulations in a similar microdiffraction experiment. Furthermore, these results suggest a general method for manipulating and orienting mesoscopic structures of weakly ordered complex fluids other than DNA–membrane complexes. This process can be automated using standard micromanipulator technology routinely used for *in vitro* fertilization.

In summary, we have found evidence for local molecular alignment within the mesoscopic fibers of DNA–membrane complexes using microdiffraction at the APS. Moreover, it

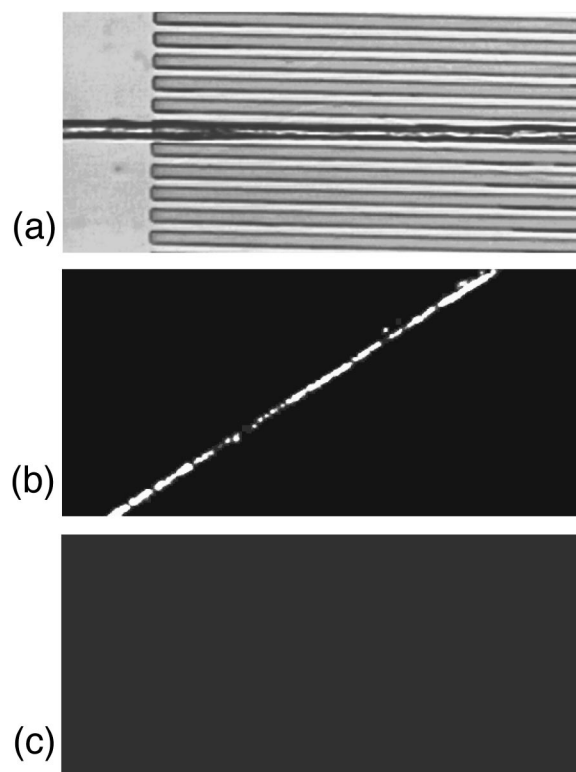


FIG. 4. (a) Lithographic channel array with an isolated fiber of DNA–membrane complexes positioned in one of the 5 \mu m wide channel depressions, imaged under direct illumination using an optical microscope. (b), (c) Rotation of the same fiber using the same magnification between crossed polarizers. Total extinction can be observed in (c). The images have been digitized using National Institute of Health software.

has been demonstrated that the mesoscopic structure of the DNA–membrane complex can be manipulated using lithographic microchannel arrays. Future work includes solution templating of the aligned fibers, as well as the employment of microchannels with widths approaching the persistence length of DNA.

The authors thank H. Kim and B. Lai for their technical assistance. This work was supported by NSF-DMR-9625977, NSF-DMR-9624091, PRF-31352-AC7, and ONR Grant No. N00014-93-1-0269. The Material Research Laboratory at U.C., Santa Barbara is supported by NSF-DMR-9632716. The APS is supported by the DOE, Basic Energy Sciences, Office of Energy Research, under Contract No. 11-31-109-Eng-38.

¹For a review, see R. G. Crystal, *Science* **270**, 404 (1995).

²J. O. Rädler, I. Koltover, T. Salditt, and C. R. Safinya, *Science* **275**, 810 (1997).

³T. Salditt, I. Koltover, J. O. Rädler, and C. R. Safinya, *Phys. Rev. Lett.* **79**, 2582 (1997).

⁴I. Koltover, T. Salditt, J. O. Rädler, and C. R. Safinya, *Science* **281**, 78 (1998).

⁵G. S. Manning, *J. Chem. Phys.* **51**, 924 (1969).

⁶C. T. Kresge, M. E. Leonowitz, W. J. Roth, J. C. Vartuli, and J. S. Beck, *Nature (London)* **359**, 710 (1992).

⁷N. K. Raman, M. T. Anderson, and C. J. Brinker, *Chem. Mater.* **8**, 1682 (1996).

⁸S. H. Tolbert, A. Firouzi, G. D. Stucky, and B. F. Chmelka, *Science* **278**, 264 (1997).

⁹W. Yun, B. Lai, D. Shu, A. Khounsary, Z. Cai, J. Barraza, and D. Legnini, *Rev. Sci. Instrum.* **67**, 3373 (1996).